July /August 2020
ISSN: 0193-4120 Page No. 6801-6817

Design and Simulation of Decoder and Encoder Device

Arun G[1], Dr. A. S. Rathore[2], Dr. Sudhir N Shelke[3]

[1]Research Scholar, Department of Electronics & Communication Engineering, Sri Satya Sai University of Technology & Medical Sciences, Sehore, M.P.

[2] Research Guide, Department of Electronics & Communication Engineering, Sri Satya Sai University of Technology & Medical Sciences, Sehore, M.P.

[3]Principal, Guru Nanak Institute of Technology, Nagpur

Article Info
Volume 83
Page Number: 6801-6817
Publication Issue:
July /August 2020

Article History
Article Received :*25 April 2020*
Revised: *19 May 2020*
Accepted: *22 June 2020*
Publication: *23 August 2020*

Abstract

The mechanics of the Mach-Zehnder interferometer (MZI) and the beam propagation technique (BPM) has been covered. The cascade of MZIs has been proposed here as a means of designing certain photonics devices. As photonics integrated circuits rely on optical waveguides and switching devices, these elements must be carefully designed. In this article, design of decoder and encoder device has been discussed.

Keywords: Design, Decoder, Encoder, Device

INTRODUCTION:

In the field of (optical) communications, they play a role in both multiplexing and de-multiplexing signals. These technologies have recently found practical use in a wide variety of contexts, including but not limited to optical communication, data transmission, video transmission, and optical networking. As optical waveguides and switching devices are so important to wavelength division multiplexing (WDM) systems, they have recently received a lot of research interest.

Design of Decoder Circuit Using Mzis:

The decoder is designed using the electro-optic action within the lithium niobate of MZI. We begin by developing a 2-to-4-line decoder, and then we suggest a 3-to-8-line decoder that uses MZI cascading.

Design of 2-4 line decoder:

Figure 1 (a) depicts the digital circuit of a 2-4 line decoder, whereas Figure1 (b) displays the design of an optical 2-4 line decoder based on MZIs. The optical signal is given as a continuous waveform to the MZI1 receiver. Next-stage MZIs have their input terminals connected to the output terminals of the prior stages (seen from Figure 1 b). Terminals 1 and 2 of MZI2's output are connected to terminal 1 of MZI4 and terminal 1 of MZI3, respectively. Electrode 2 of MZI1 receives the enable control signal (E), whereas electrode 2 of MZI2 receives the A signal, and electrodes 3 and 4 of MZI4 receive the B signal. The output of the decoder circuit is taken from the terminals labelled as "output" on MZI3 and MZI4 as O_0, O_1, O_2, and O_3.

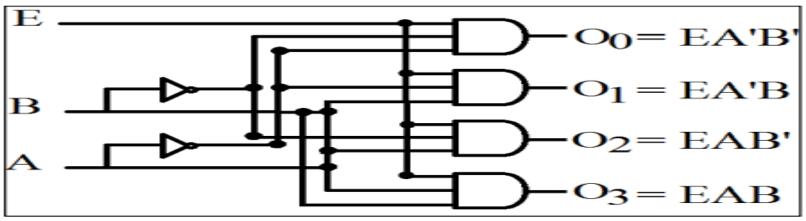

Figure 1 (a): Digital circuit of 2-4 line decoder

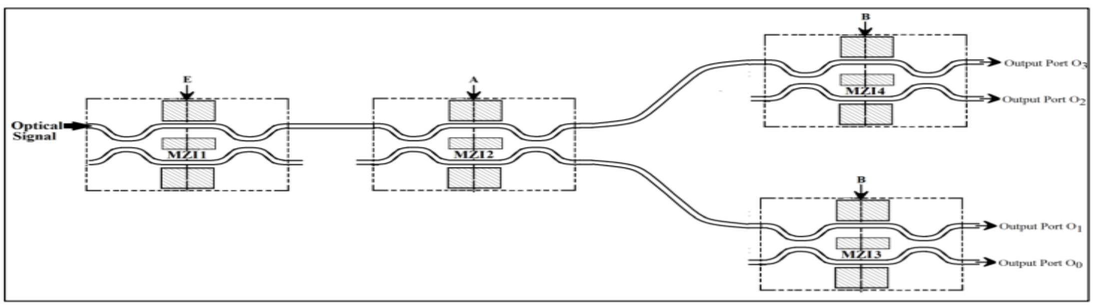

Figure 2 (b): Design of 2-4 line optical decoder

Table 1 Truth table of 2-4 line decoder

Control Signals			Optical propagation at output ports			
E	A	B	Output O_0	Output O_1	Output O_2	Output O_3
0	X	X	0	0	0	0
1	0	0	1	0	0	0
1	0	1	0	1	0	0
1	1	0	0	0	1	0
1	1	1	0	0	0	1

Mathematical formulation for 2-4 line decoder circuit:

The output terminals of MZI3 and MZI4 must be connected to power in order for the 2-4 line decoder to function. This means that the power at the terminals (O0, O1, O2, and O3) is determined by applying the formula for a single stage of MZI (Eqs. (12) and (13). We can write the output O_0at output terminal two of MZI3 as;

$$O_{0_{MZI3}} = \begin{bmatrix} \left\{-je^{-j(\varphi_{oMZI1})}\sin\left(\frac{\Delta\varphi_{MZI1}}{2}\right)\right\} \\ \left\{je^{-j(\varphi_{oMZI2})}\cos\left(\frac{\Delta\varphi_{MZI2}}{2}\right)\right\} \\ \left\{je^{-j(\varphi_{oMZI3})}\cos\left(\frac{\Delta\varphi_{MZI3}}{2}\right)\right\} \end{bmatrix} E_{in}$$

$$\frac{O_{0MZI3}}{E_{in}} = \begin{bmatrix} \left\{-je^{-j(\varphi_{oMZI1})}\sin\left(\frac{\Delta\varphi_{MZI1}}{2}\right)\right\} \\ \left\{je^{-j(\varphi_{oMZI2})}\cos\left(\frac{\Delta\varphi_{MZI2}}{2}\right)\right\} \\ \left\{je^{-j(\varphi_{oMZI3})}\cos\left(\frac{\Delta\varphi_{MZI3}}{2}\right)\right\} \end{bmatrix}$$

$$O_0 = \left|\frac{O_{0MZI3}}{E_{in}}\right|^2 = sin^2\left(\frac{\Delta\emptyset_{MZI1}}{2}\right)cos^2\left(\frac{\Delta\emptyset_{MZI2}}{2}\right)cos^2\left(\frac{\Delta\emptyset_{MZI3}}{2}\right)$$

Assume that O_1 is the signal coming out of MZI3's first output terminal.

$$O_{1_{MZI3}} = \begin{bmatrix} \left\{-je^{-j(\varphi_{oMZI1})}\sin\left(\frac{\Delta\varphi_{MZI1}}{2}\right)\right\} \\ \left\{je^{-j(\varphi_{oMZI2})}\cos\left(\frac{\Delta\varphi_{MZI2}}{2}\right)\right\} \\ \left\{-je^{-j(\varphi_{oMZI3})}\sin\left(\frac{\Delta\varphi_{MZI3}}{2}\right)\right\} \end{bmatrix} E_{in}$$

$$\frac{O_{1MZI3}}{E_{in}} = \begin{bmatrix} \left\{-je^{-j(\varphi_{oMZI1})}\sin\left(\frac{\Delta\varphi_{MZI1}}{2}\right)\right\} \\ \left\{je^{-j(\varphi_{oMZI2})}\cos\left(\frac{\Delta\varphi_{MZI2}}{2}\right)\right\} \\ \left\{-je^{-j(\varphi_{oMZI3})}\sin\left(\frac{\Delta\varphi_{MZI3}}{2}\right)\right\} \end{bmatrix}$$

$$O_1 = \left|\frac{O_{1MZI3}}{E_{in}}\right|^2 = sin^2\left(\frac{\Delta\emptyset_{MZI1}}{2}\right)cos^2\left(\frac{\Delta\emptyset_{MZI2}}{2}\right)sin^2\left(\frac{\Delta\emptyset_{MZI3}}{2}\right)$$

The O_2 output from MZI4's second terminal

$$O_{2_{MZI4}} = \begin{bmatrix} \left\{-je^{-j(\varphi_{oMZI1})}\sin\left(\frac{\Delta\varphi_{MZI1}}{2}\right)\right\} \\ \left\{-je^{-j(\varphi_{oMZI2})}\sin\left(\frac{\Delta\varphi_{MZI2}}{2}\right)\right\} \\ \left\{je^{-j(\varphi_{oMZI4})}\cos\left(\frac{\Delta\varphi_{MZI4}}{2}\right)\right\} \end{bmatrix} E_{in}$$

$$\frac{O_{2MZI4}}{E_{in}} == \begin{bmatrix} \left\{-je^{-j(\varphi_{oMZI1})}\sin\left(\frac{\Delta\varphi_{MZI1}}{2}\right)\right\} \\ \left\{-je^{-j(\varphi_{oMZI2})}\sin\left(\frac{\Delta\varphi_{MZI2}}{2}\right)\right\} \\ \left\{je^{-j(\varphi_{oMZI4})}\cos\left(\frac{\Delta\varphi_{MZI4}}{2}\right)\right\} \end{bmatrix}$$

$$O_2 = \left|\frac{O_{2MZI4}}{E_{in}}\right|^2 = sin^2\left(\frac{\Delta\emptyset_{MZI1}}{2}\right)sin^2\left(\frac{\Delta\emptyset_{MZI2}}{2}\right)cos^2\left(\frac{\Delta\emptyset_{MZI4}}{2}\right)$$

The MZI4 output O_3 at terminal one as;

$$O_{3_{MZI4}} = \begin{bmatrix} \left\{-je^{-j(\varphi_{oMZI1})}\sin\left(\frac{\Delta\varphi_{MZI1}}{2}\right)\right\} \\ \left\{-je^{-j(\varphi_{oMZI2})}\sin\left(\frac{\Delta\varphi_{MZI2}}{2}\right)\right\} \\ \left\{-je^{-j(\varphi_{oMZI4})}\sin\left(\frac{\Delta\varphi_{MZI4}}{2}\right)\right\} \end{bmatrix} E_{in}$$

$$\frac{O_{3MZI4}}{E_{in}} == \begin{bmatrix} \left\{-je^{-j(\varphi_{oMZI1})}\sin\left(\frac{\Delta\varphi_{MZI1}}{2}\right)\right\} \\ \left\{-je^{-j(\varphi_{oMZI2})}\sin\left(\frac{\Delta\varphi_{MZI2}}{2}\right)\right\} \\ \left\{-je^{-j(\varphi_{oMZI4})}\sin\left(\frac{\Delta\varphi_{MZI4}}{2}\right)\right\} \end{bmatrix}$$

$$O_3 = \left|\frac{O_{3MZI4}}{E_{in}}\right|^2 = sin^2\left(\frac{\Delta\emptyset_{MZI1}}{2}\right)sin^2\left(\frac{\Delta\emptyset_{MZI2}}{2}\right)sin^2\left(\frac{\Delta\emptyset_{MZI4}}{2}\right)$$

The formula for determining the phase difference in MZI is:

$$\left.\begin{aligned} \Delta\emptyset_{MZI1} &= \emptyset_{11} - \emptyset_{12} \\ \Delta\emptyset_{MZI2} &= \emptyset_{21} - \emptyset_{22} \\ \Delta\emptyset_{MZI3} &= \emptyset_{31} - \emptyset_{32} \\ \Delta\emptyset_{MZI4} &= \emptyset_{41} - \emptyset_{42} \end{aligned}\right\} \qquad \left.\begin{aligned} \emptyset_{11} &= \frac{\pi}{V\pi}\,A\,, \emptyset_{12} = \frac{\pi}{V\pi}\,B \\ \emptyset_{21} &= \frac{\pi}{V\pi}\,A\,, \emptyset_{22} = \frac{\pi}{V\pi}\,B \\ \emptyset_{31} &= \frac{\pi}{V\pi}\,A\,, \emptyset_{32} = \frac{\pi}{V\pi}\,B \\ \emptyset_{41} &= \frac{\pi}{V\pi}\,A\,, \emptyset_{42} = \frac{\pi}{V\pi}\,B \end{aligned}\right\}$$

The results of MATLAB simulations of a 2-4 line decoder with various 'AB' (i.e. 00, 01, 10, and 11) control signal combinations are displayed in Figure2. When the A and B control signals are both zero, the output O_0 is achieved. Similarly, Table 1 displays the outputs O_1, O_2, and O_3 that are generated by varying the control signals. The first column displays the active enable signal, while the second and third columns display the active A and B control signals. The decoder's output at its various ends is shown in the final four columns.

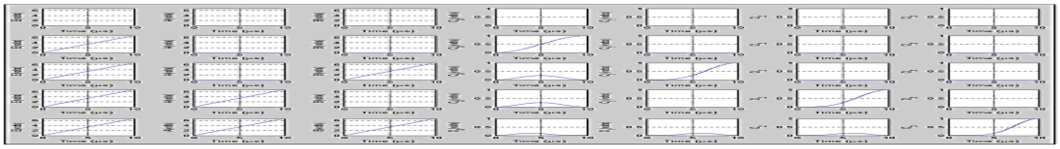

Figure 3. MATLAB simulation result of 2-4 line decoder

Design of 2-4 line decoder using BPM:

The design of a 2-4 line decoder circuit is shown in Figure 3. The circuit architecture here makes use of four MZIs. MZI1 receives an optical signal at its input terminal 1. One of MZI2 input terminals is connected to MZI1's output terminal 1. First input terminals of MZI4 and MZI3 are connected to MZI2's first and second inputs, respectively. For MZI1, E is sent, for MZI2 A, and for MZI3 and MZI4 B is supplied.

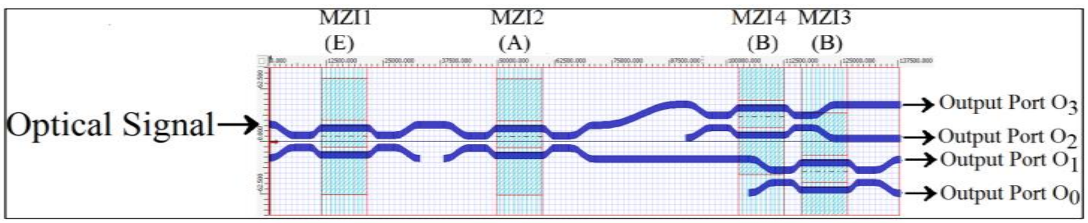

Figure 3 Design of 2-4 line decoder

In order to simulate the performance of the suggested device, the following simulation parameters have been obtained in Opti-BPM software.

Table 2 Simulation parameters for 2-4 line decoder (Raghuwanshi et al. 2013)

Parameters	Properties
Wave length	1.3 μm
Polarization	Transverse Magnetic
BPM Solver	Paraxial
Propagation Step	1.3
Scheme parameter	0.5
Boundary condition	Transparent boundary condition (TBC)
Mesh points	2500

The possible permutations of the three control signals (E, A and B) shown in Figure 1 are considered and analyzed in detail in the following section on the proposed design:

Case 1: $E = 0$, $A = X$ and $B = X$

Signal (optical) is applied at MZI1 as shown in Figure 4. An enable (E) signal is applied to MZI1's electrode 2, a control (A) signal is applied to MZI2's electrode 2, and a bias (B) signal is applied to MZI2 and MZI4. Signal (optical) appears at output terminal two of MZI1 when zero voltage is applied at electrode two ($E = 0$). That's why the signal doesn't go on to the subsequent MZIs. This

July /August 2020
ISSN: 0193-4120 Page No. 6801-6817

indicates that the control signals A and B have no effect on the decoder's output because the output at terminals O_0 through O_3 is 0 (Figure 4).

Case 2: E = 1, A = 0 and B = 0

In this case, the signal (optical) will be sent at MZI2 when the voltage is high at electrode two (control signal E = 1). Output appears at output terminal two, which is linked to input terminal one of MZI3, when control signal A is zero (voltage zero at electrode two of MZI2). Signal (optical) transfer occurs at terminal O_0, where the control signal B is also 0. Hence, all but the O_0 terminal will have a zero output (Figure 4).

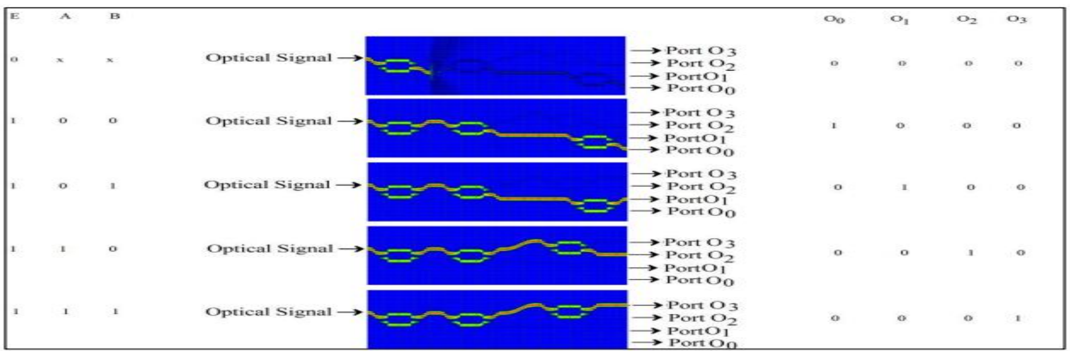

Figure 4. Verification of truth table of decoder using beam propagation method

Case 3: E = 1, A = 0 and B = 1

By definition, when control signal A is low, signal arrives at output terminal two of MZI2, and vice versa when enable signal E is high, indicating that output will be received at output terminal one of MZI1. To advance the optical signal at terminal $O1$ from MZI2, a control signal (B = 1) is provided to electrode two of MZI3. By doing so, we make it such that just the $O1$ output terminal is getting the signal (optical), while the other endpoints are not.

Case 4: E = 1, A = 1 and B = 0

Since enable signal E is high, the output will be sent to MZI1's terminal one, and since control signal A is likewise high, MZI2's terminal one will receive the signal as well. When the B control signal is at its minimum at electrode two of MZI4, the optical signal is sent to terminal $O2$. It causes a rise in $O2$ at the terminal output.

Case 5: E = 1, A = 1 and B = 1

Signal is provided to input terminal one of MZI2 while enable signal E = 1 is applied to electrode two of MZI1. A High signal is received from MZI2's first output terminal when control signal is A high. When an input signal is applied to MZI4's control signal B with a high level, the output signal is sent to terminal O_3. We use a truth table to back up our findings.

TEST Engineering & Management
July /August 2020
ISSN: 0193-4120 Page No. 6801-6817

Design of 3-8 Line Decoder:

Both the digital circuit of a 3-8 line decoder (Figure 5 (a)) and its optical counterpart (Figure 5 (b)) are depicted. To create the 3-8 line decoder, eight MZIs are utilised. Power is sent from a CW optical source using MZI1's terminal one input. After this, MZI2 takes the optical data sent from MZI1 and transfers it to MZI3 and MZI4. The MZI3 outputs are connected to the MZI6 and MZI5 inputs. The MZI4 outputs are connected to the first inputs of the MZI8 and MZI7.

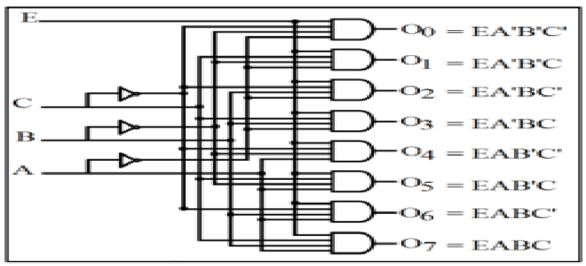

Figure 5 (a): Digital circuit of 3-8 line decoder

Decoder functioning is determined by an enable (E) signal applied to MZI1. MZI2 receives control signal A, MZI3 and MZI4 get signal B, while MZI5, MZI6, MZI7, and MZI8 get signal C. For the sake of this discussion, the output terminals of MZI5, MZI6, MZI7, and MZI8 will be referred to as $O0$ through $O7$. Table 3 displays the truth table for the 3-8 line decoder.

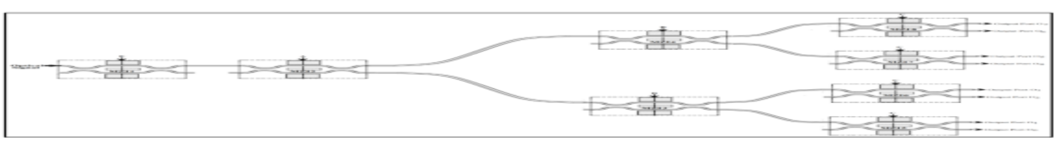

Figure 6 (b): Schematic diagram of 3-8 line optical decoder

Table 3 Truth table of 3-8-line decoder

Control Signals				Optical propagation at various output terminal (OT)							
E	A	B	C	OT O_0	OT O_1	OT O_2	OT O_3	OT O_4	OT O_5	OT O_6	OT O_7
0	X	X	X	0	0	0	0	0	0	0	0
1	0	0	0	1	0	0	0	0	0	0	0
1	0	0	1	0	1	0	0	0	0	0	0
1	0	1	0	0	0	1	0	0	0	0	0
1	0	1	1	0	0	0	1	0	0	0	0
1	1	0	0	0	0	0	0	1	0	0	0
1	1	0	1	0	0	0	0	0	1	0	0
1	1	1	0	0	0	0	0	0	0	1	0
1	1	1	1	0	0	0	0	0	0	0	1

July /August 2020
ISSN: 0193-4120 Page No. 6801-6817

Mathematical formulation of 3-8 line decoder:

In order to analytically derive the normalized power at the output terminals of MZIs, the expression of a single stage MZI is used. The MZI5 normalized output power at terminal two is calculated as:

$$O_{0_{MZI5}} = \begin{bmatrix} \left\{-je^{-j(\varphi_{oMZI1})}\sin\left(\frac{\Delta\varphi MZI1}{2}\right)\right\} \\ \left\{je^{-j(\varphi_{oMZI2})}\cos\left(\frac{\Delta\varphi MZI2}{2}\right)\right\} \\ \left\{je^{-j(\varphi_{oMZI3})}\cos\left(\frac{\Delta\varphi MZI3}{2}\right)\right\} \\ \left\{je^{-j(\varphi_{oMZI5})}\cos\left(\frac{\Delta\varphi MZI5}{2}\right)\right\} \end{bmatrix} E_{in}$$

$$\frac{O_{0MZI5}}{E_{in}} = \begin{bmatrix} \left\{-je^{-j(\varphi_{oMZI1})}\sin\left(\frac{\Delta\varphi MZI1}{2}\right)\right\} \\ \left\{je^{-j(\varphi_{oMZI2})}\cos\left(\frac{\Delta\varphi MZI2}{2}\right)\right\} \\ \left\{je^{-j(\varphi_{oMZI3})}\cos\left(\frac{\Delta\varphi MZI3}{2}\right)\right\} \\ \left\{je^{-j(\varphi_{oMZI5})}\cos\left(\frac{\Delta\varphi MZI5}{2}\right)\right\} \end{bmatrix}$$

$$O_0 = \left|\frac{O_{0MZI5}}{E_{in}}\right|^2 = \sin^2\left(\frac{\Delta\emptyset MZI1}{2}\right)\cos^2\left(\frac{\Delta\emptyset MZI2}{2}\right)\cos^2\left(\frac{\Delta\emptyset MZI3}{2}\right)\cos^2\left(\frac{\Delta\emptyset MZI5}{2}\right)$$

Below is the formula for MZI5's normalized power output at terminal one:

$$O_{1_{MZI5}} = \begin{bmatrix} \left\{-je^{-j(\varphi_{oMZI1})}\sin\left(\frac{\Delta\varphi MZI1}{2}\right)\right\} \\ \left\{je^{-j(\varphi_{oMZI2})}\cos\left(\frac{\Delta\varphi MZI2}{2}\right)\right\} \\ \left\{je^{-j(\varphi_{oMZI3})}\cos\left(\frac{\Delta\varphi MZI3}{2}\right)\right\} \\ \left\{-je^{-j(\varphi_{oMZI5})}\sin\left(\frac{\Delta\varphi MZI5}{2}\right)\right\} \end{bmatrix} E_{in}$$

$$\frac{O_{1MZI5}}{E_{in}} = \begin{bmatrix} \left\{-je^{-j(\varphi_{oMZI1})}\sin\left(\frac{\Delta\varphi MZI1}{2}\right)\right\} \\ \left\{je^{-j(\varphi_{oMZI2})}\cos\left(\frac{\Delta\varphi MZI2}{2}\right)\right\} \\ \left\{je^{-j(\varphi_{oMZI3})}\cos\left(\frac{\Delta\varphi MZI3}{2}\right)\right\} \\ \left\{-je^{-j(\varphi_{oMZI5})}\sin\left(\frac{\Delta\varphi MZI5}{2}\right)\right\} \end{bmatrix}$$

$$O_1 = \left|\frac{O_{1MZI5}}{E_{in}}\right|^2 = \sin^2\left(\frac{\Delta\emptyset MZI1}{2}\right)\cos^2\left(\frac{\Delta\emptyset MZI2}{2}\right)\cos^2\left(\frac{\Delta\emptyset MZI3}{2}\right)\sin^2\left(\frac{\Delta\emptyset MZI5}{2}\right)$$

Using terminal two of MZI6's output, we can calculate the power normalized output as:

$$O_{2_{MZI6}} = \begin{bmatrix} \left\{-je^{-j(\varphi_{oMZI1})}\sin\left(\frac{\Delta\varphi MZI1}{2}\right)\right\} \\ \left\{je^{-j(\varphi_{oMZI2})}\cos\left(\frac{\Delta\varphi MZI2}{2}\right)\right\} \\ \left\{-je^{-j(\varphi_{oMZI3})}\sin\left(\frac{\Delta\varphi MZI3}{2}\right)\right\} \\ \left\{je^{-j(\varphi_{oMZI6})}\cos\left(\frac{\Delta\varphi MZI6}{2}\right)\right\} \end{bmatrix} E_{in}$$

$$\frac{O_{2MZI6}}{E_{in}} = \begin{bmatrix} \left\{-je^{-j(\varphi_{oMZI1})}\sin\left(\frac{\Delta\varphi MZI1}{2}\right)\right\} \\ \left\{je^{-j(\varphi_{oMZI2})}\cos\left(\frac{\Delta\varphi MZI2}{2}\right)\right\} \\ \left\{-je^{-j(\varphi_{oMZI3})}\sin\left(\frac{\Delta\varphi MZI3}{2}\right)\right\} \\ \left\{je^{-j(\varphi_{oMZI6})}\cos\left(\frac{\Delta\varphi MZI6}{2}\right)\right\} \end{bmatrix}$$

$$O_2 = \left|\frac{O_{2MZI6}}{E_{in}}\right|^2 = \sin^2\left(\frac{\Delta\emptyset MZI1}{2}\right)\cos^2\left(\frac{\Delta\emptyset MZI2}{2}\right)\sin^2\left(\frac{\Delta\emptyset MZI3}{2}\right)\cos^2\left(\frac{\Delta\emptyset MZI6}{2}\right)$$

The MZI6 normalized power at terminal one of the device's output is calculated as:

$$O_{3_{MZI6}} = \begin{bmatrix} \left\{-je^{-j(\varphi_{oMZI1})}\sin\left(\frac{\Delta\varphi MZI1}{2}\right)\right\} \\ \left\{je^{-j(\varphi_{oMZI2})}\cos\left(\frac{\Delta\varphi MZI2}{2}\right)\right\} \\ \left\{-je^{-j(\varphi_{oMZI3})}\sin\left(\frac{\Delta\varphi MZI3}{2}\right)\right\} \\ \left\{-je^{-j(\varphi_{oMZI6})}\sin\left(\frac{\Delta\varphi MZI6}{2}\right)\right\} \end{bmatrix} E_{in}$$

$$\frac{O_{3MZI6}}{E_{in}} = \begin{bmatrix} \left\{-je^{-j(\varphi_{oMZI1})}\sin\left(\frac{\Delta\varphi MZI1}{2}\right)\right\} \\ \left\{je^{-j(\varphi_{oMZI2})}\cos\left(\frac{\Delta\varphi MZI2}{2}\right)\right\} \\ \left\{-je^{-j(\varphi_{oMZI3})}\sin\left(\frac{\Delta\varphi MZI3}{2}\right)\right\} \\ \left\{-je^{-j(\varphi_{oMZI6})}\sin\left(\frac{\Delta\varphi MZI6}{2}\right)\right\} \end{bmatrix}$$

$$O_3 = \left|\frac{O_{3MZI6}}{E_{in}}\right|^2 = \sin^2\left(\frac{\Delta\emptyset MZI1}{2}\right)\cos^2\left(\frac{\Delta\emptyset MZI2}{2}\right)\sin^2\left(\frac{\Delta\emptyset MZI3}{2}\right)\sin^2\left(\frac{\Delta\emptyset MZI6}{2}\right)$$

In order to calculate the normalized power at MZI7's terminal two, we have:

$$O_{4_{MZI7}} = \begin{bmatrix} \left\{-je^{-j(\varphi_{oMZI1})}\sin\left(\frac{\Delta\varphi MZI1}{2}\right)\right\} \\ \left\{-je^{-j(\varphi_{oMZI2})}\sin\left(\frac{\Delta\varphi MZI2}{2}\right)\right\} \\ \left\{je^{-j(\varphi_{oMZI4})}\cos\left(\frac{\Delta\varphi MZI4}{2}\right)\right\} \\ \left\{je^{-j(\varphi_{oMZI7})}\cos\left(\frac{\Delta\varphi MZI7}{2}\right)\right\} \end{bmatrix} E_{in}$$

$$\frac{O_{4MZI7}}{E_{in}} = \begin{bmatrix} \left\{-je^{-j(\varphi_{oMZI1})}\sin\left(\frac{\Delta\varphi MZI1}{2}\right)\right\} \\ \left\{-je^{-j(\varphi_{oMZI2})}\sin\left(\frac{\Delta\varphi MZI2}{2}\right)\right\} \\ \left\{je^{-j(\varphi_{oMZI4})}\cos\left(\frac{\Delta\varphi MZI4}{2}\right)\right\} \\ \left\{je^{-j(\varphi_{oMZI7})}\cos\left(\frac{\Delta\varphi MZI7}{2}\right)\right\} \end{bmatrix}$$

July /August 2020
ISSN: 0193-4120 Page No. 6801-6817

$$O_4 = \left|\frac{O_{4MZI7}}{E_{in}}\right|^2 = sin^2\left(\frac{\Delta\Phi_{MZI1}}{2}\right) sin^2\left(\frac{\Delta\Phi_{MZI2}}{2}\right) cos^2\left(\frac{\Delta\Phi_{MZI4}}{2}\right) cos^2\left(\frac{\Delta\Phi_{MZI7}}{2}\right)$$

The output power, normalized, from MZI7's terminal one is as follows:

$$O_{5MZI7} = \begin{bmatrix} \left\{-je^{-j(\varphi_{oMZI1})}\sin\left(\frac{\Delta\varphi MZI1}{2}\right)\right\} \\ \left\{-je^{-j(\varphi_{oMZI2})}\sin\left(\frac{\Delta\varphi MZI2}{2}\right)\right\} \\ \left\{je^{-j(\varphi_{oMZI4})}\cos\left(\frac{\Delta\varphi MZI4}{2}\right)\right\} \\ \left\{-je^{-j(\varphi_{oMZI7})}\sin\left(\frac{\Delta\varphi MZI7}{2}\right)\right\} \end{bmatrix} E_{in}$$

$$\frac{O_{5MZI7}}{E_{in}} = \begin{bmatrix} \left\{-je^{-j(\varphi_{oMZI1})}\sin\left(\frac{\Delta\varphi MZI1}{2}\right)\right\} \\ \left\{-je^{-j(\varphi_{oMZI2})}\sin\left(\frac{\Delta\varphi MZI2}{2}\right)\right\} \\ \left\{je^{-j(\varphi_{oMZI4})}\cos\left(\frac{\Delta\varphi MZI4}{2}\right)\right\} \\ \left\{-je^{-j(\varphi_{oMZI7})}\sin\left(\frac{\Delta\varphi MZI7}{2}\right)\right\} \end{bmatrix}$$

$$O_5 = \left|\frac{O_{5MZI7}}{E_{in}}\right|^2 = sin^2\left(\frac{\Delta\Phi_{MZI1}}{2}\right) sin^2\left(\frac{\Delta\Phi_{MZI2}}{2}\right) cos^2\left(\frac{\Delta\Phi_{MZI4}}{2}\right) sin\left(\frac{\Delta\Phi_{MZI7}}{2}\right)$$

The MZI8 normalized power at terminal two of the device's output is calculated as:

$$O_{6MZI8} = \begin{bmatrix} \left\{-je^{-j(\varphi_{oMZI1})}\sin\left(\frac{\Delta\varphi MZI1}{2}\right)\right\} \\ \left\{-je^{-j(\varphi_{oMZI2})}\sin\left(\frac{\Delta\varphi MZI2}{2}\right)\right\} \\ \left\{-je^{-j(\varphi_{oMZI4})}\sin\left(\frac{\Delta\varphi MZI4}{2}\right)\right\} \\ \left\{je^{-j(\varphi_{oMZI8})}\cos\left(\frac{\Delta\varphi MZI8}{2}\right)\right\} \end{bmatrix} E_{in}$$

$$\frac{O_{6MZI8}}{E_{in}} = \begin{bmatrix} \left\{-je^{-j(\varphi_{oMZI1})}\sin\left(\frac{\Delta\varphi MZI1}{2}\right)\right\} \\ \left\{-je^{-j(\varphi_{oMZI2})}\sin\left(\frac{\Delta\varphi MZI2}{2}\right)\right\} \\ \left\{-je^{-j(\varphi_{oMZI4})}\sin\left(\frac{\Delta\varphi MZI4}{2}\right)\right\} \\ \left\{je^{-j(\varphi_{oMZI8})}\cos\left(\frac{\Delta\varphi MZI8}{2}\right)\right\} \end{bmatrix}$$

$$O_6 = \left|\frac{O_{6MZI8}}{E_{in}}\right|^2 = sin^2\left(\frac{\Delta\Phi_{MZI1}}{2}\right) sin^2\left(\frac{\Delta\Phi_{MZI2}}{2}\right) sin^2\left(\frac{\Delta\Phi_{MZI4}}{2}\right) cos^2\left(\frac{\Delta\Phi_{MZI8}}{2}\right)$$

MZI8's terminal one output power is normalized as follows:

$$O_{7MZI8} = \begin{bmatrix} \left\{-je^{-j(\varphi_{oMZI1})}\sin\left(\frac{\Delta\varphi MZI1}{2}\right)\right\} \\ \left\{-je^{-j(\varphi_{oMZI2})}\sin\left(\frac{\Delta\varphi MZI2}{2}\right)\right\} \\ \left\{-je^{-j(\varphi_{oMZI4})}\sin\left(\frac{\Delta\varphi MZI4}{2}\right)\right\} \\ \left\{-je^{-j(\varphi_{oMZI8})}\sin\left(\frac{\Delta\varphi MZI8}{2}\right)\right\} \end{bmatrix} E_{in}$$

$$\frac{O_{7MZI8}}{E_{in}} = \begin{bmatrix} \left\{-je^{-j(\varphi_{oMZI1})}\sin\left(\frac{\Delta\varphi MZI1}{2}\right)\right\} \\ \left\{-je^{-j(\varphi_{oMZI2})}\sin\left(\frac{\Delta\varphi MZI2}{2}\right)\right\} \\ \left\{-je^{-j(\varphi_{oMZI4})}\sin\left(\frac{\Delta\varphi MZI4}{2}\right)\right\} \\ \left\{-je^{-j(\varphi_{oMZI8})}\sin\left(\frac{\Delta\varphi MZI8}{2}\right)\right\} \end{bmatrix}$$

$$O_7 = \left|\frac{O_{7MZI8}}{E_{in}}\right|^2 = sin^2\left(\frac{\Delta\Phi_{MZI1}}{2}\right) sin^2\left(\frac{\Delta\Phi_{MZI2}}{2}\right) sin^2\left(\frac{\Delta\Phi_{MZI4}}{2}\right) sin^2\left(\frac{\Delta\Phi_{MZI8}}{2}\right)$$

A 3-8 line decoder with comparable results to those in Figure 2 may be built in MATLAB.

Design of 3-8 line decoder using BPM:

The circuit configuration of a 3-8 line decoder is shown in Figure 6. This suggested gadget is designed with eight MZIs. An optical signal is applied to MZI1's first input terminal. The first MZI output terminal is connected to the second MZI input terminal. In this configuration, MZI2's output terminals (1 and 2) are connected to MZI4 and MZI3, respectively. Signal A is connected to MZI1, signal B is applied to MZI2, signal C is applied to MZI3, MZI4, and signal D is applied to MZI5, MZI6, MZI7, and MZI8. Enable E is supplied to electrode two of MZI1.

The suggested 3-8line decoder circuit is provided with all conceivable permutations of control signals. Detailed descriptions of the associated replies are provided below;

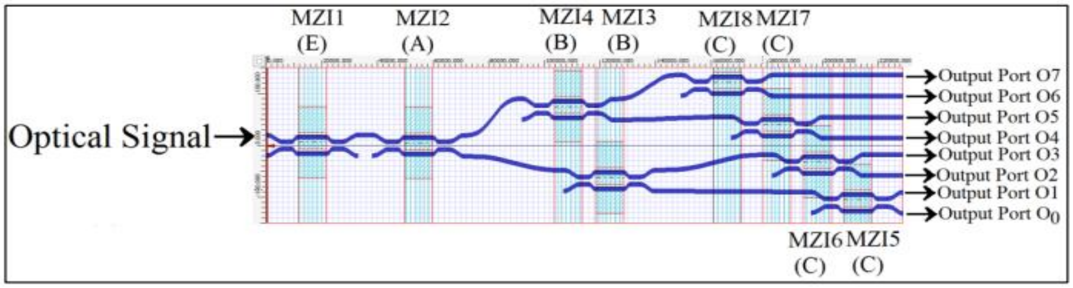

Figure 7 Layout figure of 3-8 line decoder

Case 1: E = 0, A = X, B = X, and C = X

As the voltage at MZI1's electrode two is 0 while enable signal E is also 0 in this situation, the device is in its off state. The results are shown at MZI1's terminal two for output. Currently, there are no MZIs attached to this terminal's output (Figure 6). Thus, none of terminals O_0–O_7 provides an optical signal (Figure 7a). The output is unaffected by the A, B and C control signals X is indifferent; it will be either 0 or 1).

Case 2: E = 1, A = 0, B = 0, and C = 0

When input signal E is high, MZI1 sends a signal to terminal 1. Signal transmission occurs at MZI2's second output terminal because control signal A is also low. The first input terminal of MZI3 is connected to the output of MZI2. When the voltage of control signal B is 0, the MZI3's second output terminal is used. MZI3's output is connected to MZI5's input first. Because control is zero (C = 0), MZI5's output appears at terminal O_0.

Case 3: E = 1, A = 0, B = 0, and C = 1

In the second scenario, when E = 1, A = 0, B = 0, the signal at MZI3's second output terminal was acquired, and as a result, the control signal C is high, and the second output O_2 also rose to its high state (Figure 7a).

Case 4: E = 1, A = 0, B = 1, and C = 0

The optical signal from MZI2 is acquired at MZI3's first input terminal when the control signal A is at zero. The first input terminal of MZI6 is connected to the third output terminal of MZI3. When MZI6's control signal C is at a low level, an optical signal is being transmitted to the output terminal O_2.

Case 5: E = 1, A = 0, B = 1, and C = 1

Signal (optical) obtained at MZI1 terminal one when control signal E is strong. When terminal two of MZI2's output is active due to a low value of control signal A, optical signals are sent. When the control signals B and C are high, the optical signal from MZI3 is sent to the output terminal O_3 of MZI6.

Case 6: E = 1, A = 1, B = 0, and C = 0

When input terminal one of MZI2 receives a signal, the enable signal E is high. If input signal A is high, the MZI4 will switch to its

July /August 2020
ISSN: 0193-4120 Page No. 6801-6817

first input. MZI7 output terminal O_4 is the signal transfer point when control signals B and C are both 0.

Case 7: E = 1, A = 1, B = 0, and C = 1

In this scenario, both the E and A control signals are high, and the optical signal is extracted from the MZI2's first output terminal through the inverter. A connection is made between MZI2's first output terminal and MZI4's second input terminal. With control signal B set to zero, the MZI7's input terminal one will begin to receive an optical signal. When the control signal C is high, the signal is sent optically to the fifth output terminal (O_5).

Case 8: E = 1, A = 1, B = 1, and C = 0

Due to the high levels of E, A and B, the optical signal from MZI1 is sent to terminal one of MZI4. Using MZI8, this terminal may connect to the internet. This signal (optical) at output terminal O_6, causes control signal C to be low.

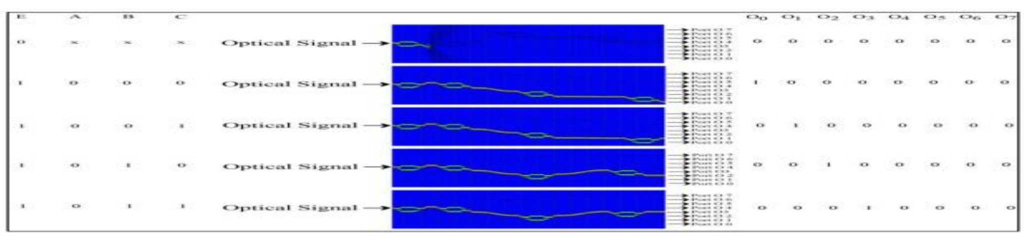

(a)

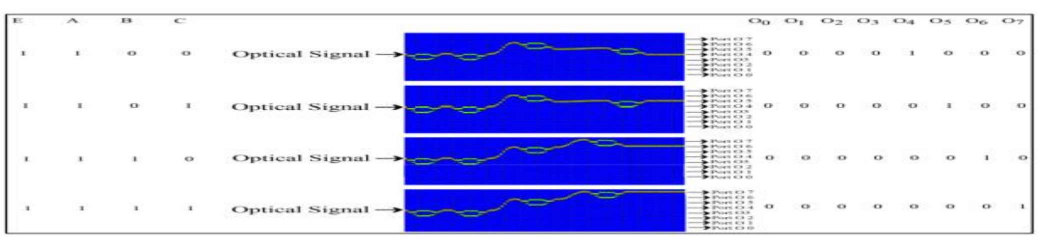

(b)

Figure 8. Simulation results of 3-8 line decoder for control signals E, A, B and C is (a): 1000 to 1011 (b): 1100 to 1111 obtained through beam propagation method

Case 9: E = 1, A = 1, B = 1, and C = 1

With all four inputs active (E, A, B and C), the optical signal is fed into MZI1's first input terminal and outputs from MZI8's seventh output terminal (O_7). When compared to the truth table shown in Table 3, our findings (Figure 7 b) hold up as expected.

Design of 4 To 2 Line Encoder Using Mzis:

July /August 2020
ISSN: 0193-4120 Page No. 6801-6817

A 4 to 2 line encoder employing MZIs is seen in Figure 8. First inputs of MZI1, MZI2, MZI3, and MZI4 are concurrently fed CW (optical) signals. That is possible because MZI1's output terminal one is connected to MZI5's input terminal one. Both MZI2 and MZI4's first output terminals are connected to MZI5's second input terminal, while MZI3 and MZI4's first output terminals are connected to MZI6's second input terminal. For the sake of this discussion, terminal two of MZI5 and MZI6 will be referred to as O_0 and O_1, respectively, for output. MZIs are controlled by the signals sent via the select lines (I_0, I_1, I_2, I_3 and E). The second electrodes of MZI1, MZI2, MZI3, and MZI4 get the control signals (I_0, I_1, I_2, I_3), whereas the second electrodes of MZI5 and MZI6 receive the enable control signal (E). Table 4 displays the truth table for the 4 to 2 line encoder.

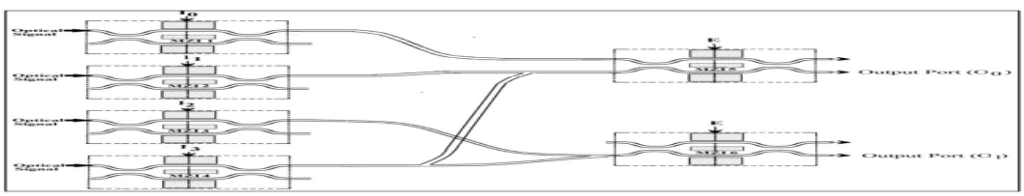

Figure 9 Conceptual diagram of 4 to 2 line encoder

Table 4 Truth table of 4 to 2 line Encoder

Control Signals					Output at different Terminals	
E	**I_0**	**I_1**	**I_2**	**I_3**	**Output (O_1)**	**Output (O_0)**
1	1	0	0	0	0	0
1	0	1	0	0	0	1
1	0	0	1	0	1	0
1	0	0	0	1	1	1

Mathematical formulation of 4 to 2 line encoder:

The power for the 4 to 2 line encoder is provided by MZI5 and MZI6's terminal two output. As a result, the following equation may be used to get the normalized power at terminal two of the output:

$$O_0 = \sin^2\left(\frac{\Delta\varnothing_{MZI1}}{2}\right)\cos^2\left(\frac{\Delta\varnothing_{MZI5}}{2}\right) + \sin^2\left(\frac{\Delta\varnothing_{MZI2}}{2}\right)\sin^2\left(\frac{\Delta\varnothing_{MZI5}}{2}\right) + \sin^2\left(\frac{\Delta\varnothing_{MZI4}}{2}\right)\sin^2\left(\frac{\Delta\varnothing_{MZI5}}{2}\right)$$

$$O_1 = \sin^2\left(\frac{\Delta\varnothing_{MZI3}}{2}\right)\sin^2\left(\frac{\Delta\varnothing_{MZI6}}{2}\right) + \sin^2\left(\frac{\Delta\varnothing_{MZI4}}{2}\right)\sin^2\left(\frac{\Delta\varnothing_{MZI6}}{2}\right)$$

The formula for determining the phase difference in MZI is:

$$\left.\begin{aligned}
\Delta\varnothing_{MZI1} &= \varnothing_{11} - \varnothing_{12}\\
\Delta\varnothing_{MZI2} &= \varnothing_{21} - \varnothing_{22}\\
\Delta\varnothing_{MZI3} &= \varnothing_{31} - \varnothing_{32}\\
\Delta\varnothing_{MZI4} &= \varnothing_{41} - \varnothing_{42}\\
\Delta\varnothing_{MZI5} &= \varnothing_{51} - \varnothing_{52}\\
\Delta\varnothing_{MZI6} &= \varnothing_{61} - \varnothing_{62}
\end{aligned}\right\}$$

The MATLAB simulation result for an optical 4 to 2 line encoder is shown in Figure 9. The first five rows detail the many

July /August 2020
ISSN: 0193-4120 Page No. 6801-6817

permutations of the enable signal and the input signals I_0, I_1, I_2, and I_3. The final two columns display the encoded output from the 4 to 2 line encoder for each of the input states.

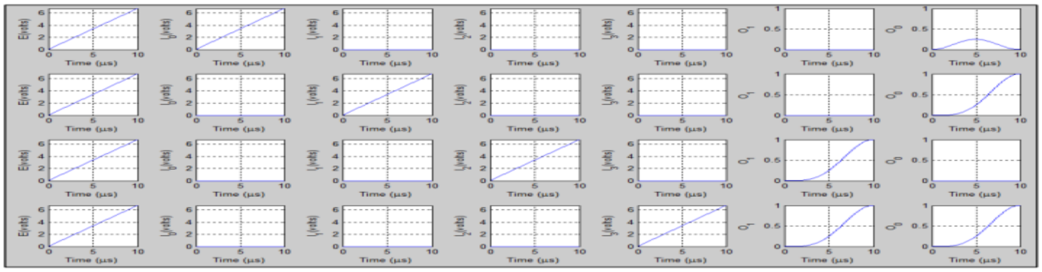

Figure 10 MATLAB simulation result of 4 to 2 line encoder

Design of 4 to 2 line encoder using BPM:

Encoder layout schematic showing 4 lines reduced to 2. One of the four MZIs receives a signal (optical) at its input terminal (MZI1, MZI2, MZI3, and MZI4). That is possible because MZI1's output terminal one is connected to MZI5's input terminal 1. Both MZI2 and MZI4's first output terminals are connected to MZI5's second input terminal, while MZI3 and MZI4's first output terminals are connected to MZI6's second input terminal. For the sake of this discussion, terminal two of MZI5 and MZI6 will be referred to as O_0 and O_1, respectively, for output. The second electrodes of MZI1, MZI2, MZI3, and MZI4 get the control signals (I_0, I_1, I_2, I_3), whereas the second electrodes of MZI5 and MZI6 receive the enable control signal (E).

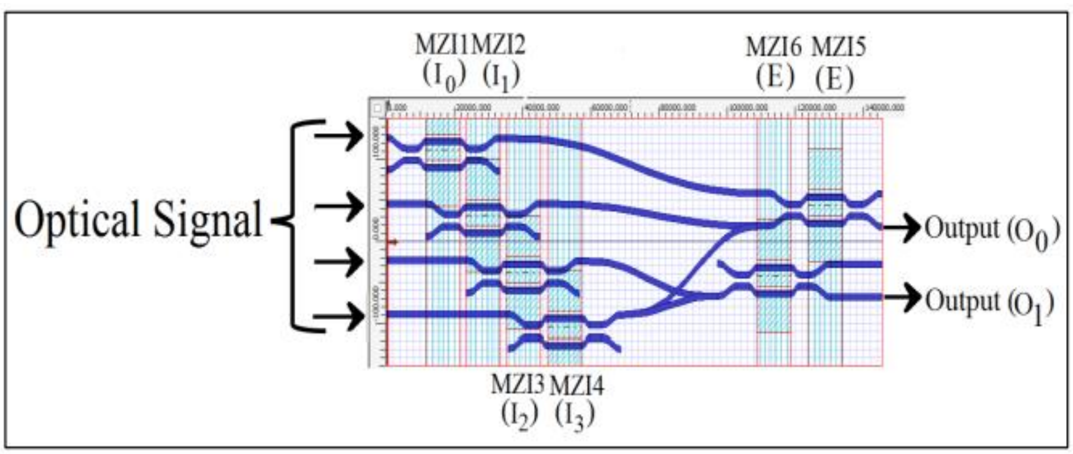

Figure 11 BPM Layout figure of 4 to 2 encoder using Mach-Zehnder interferometers

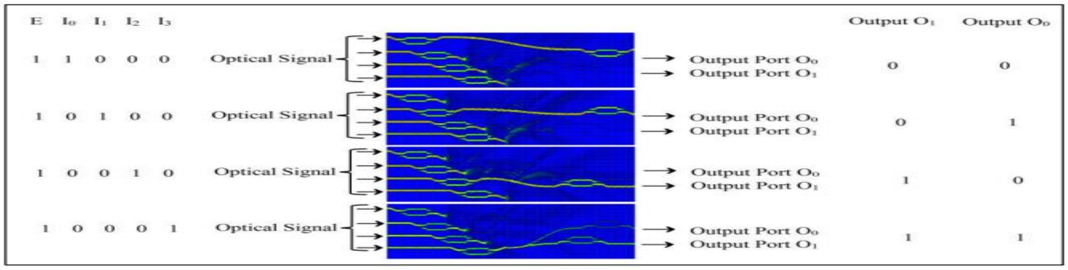

Figure 12 Results of the 4 to 2 encoder for the different combinations of the control signals ($I0$, $I1$, $I2$, $I3$ and E) obtained through the beam propagation method

In this section, we detail the proposed device's responses to the many permutations of control signals.

Case 1: $E = 1, I_0 = 1, I_1 = 0, I_2 = 0, I_3 = 0$

Input terminals of MZI1, MZI2, MZI3, and MZI4 receive optical signals, as shown in Figure 10. The MZI1's output appears at the MZI5's output terminal one, while terminal two is really the O_0 output. The optical signal may be controlled to go from one condition to another and then emerge at the correct output terminal with the aid of an enable signal. Signal (optical) at terminals O_0 and O_1 are found to be zero when high voltage is given to the center electrode of the MZI1 (control signal $I_0 = 1$). In the same way, a low voltage applied to the center electrode of MZI2, MZI3, and MZI4 (control signal $I_1 = 0$, $I_2 = 0$, $I_3 = 0$) does not affect the voltage at the output terminals O_0 and O_1, hence there is no output (Figure 11).

Case 2: $E = 1, I_0 = 0, I_1 = 1, I_2 = 0, I_3 = 0$

As can be seen in Figure 10, the output of MZI1, MZI3, and MZI4 is unaffected by the optical signal's termination within the encoder when a low voltage is given at the middle electrode (control signal $I_0 = 0$, $I_2 = 0$, $I_3 = 0$). As there is no connection between MZI2 and MZI6, applying a high voltage (6.75 V) to the centre electrode causes an optical signal to arise at terminal O_0 while the optical power at terminal O_1 drops to zero (Figure 11).

Case 3: $E = 1, I_0 = 0, I_1 = 0, I_2 = 1, I_3 = 0$

Here, the signal (optical) from MZI1, MZI2, and MZI4 is lost within the encoder in response to the control signal supplied to the second electrodes of MZI1, MZI2, MZI3, and MZI4. The control signal is $I_0 = 0$, $I_1 = 1$, $I_2 = 0$, $I_3 = 0$. When MZI3 is present, it causes the optical signal to be sent to the O_1 output terminal, but the O_0 terminal receives no power due to the fact that MZI3 is not linked to MZI5 (Figure 11).

Case 4: $E = 1, I_0 = 0, I_1 = 0, I_2 = 0, I_3 = 1$

In this scenario, the inputs can be configured such that electrode two of MZI1, MZI2, and MZI3 get a low voltage while electrode two of MZI4 receives a high voltage. Since MZI4 uses an optical transfer signal at its O_0 and O_1 terminals, this is the case. The truth table of the 4 to 2 line encoder is displayed

July /August 2020
ISSN: 0193-4120 Page No. 6801-6817

in Table 4, which verifies our results (Figure 11).

Result and Discussion:

For decoders with 2–4 lines, several performance parameters are suggested. They include the extinction ratio (ER) and the insertion loss (IL), for example. A definition of ER is:

$$ER\ (dB) = 10\log\left(\frac{P_{min}^{1}}{P_{max}^{0}}\right)$$

Optical switches with a high ER value can be toggled with ease. The relationship between the extinction ratio (ER) and the coupling ratio (CR) is shown in Figure 13, whereas Figure 12 shows the ER as a function of wavelength. The maximum extinction ratio (15.48 dB) is reached at a wavelength of 1.3 microns and a coupling ratio of 0.5.

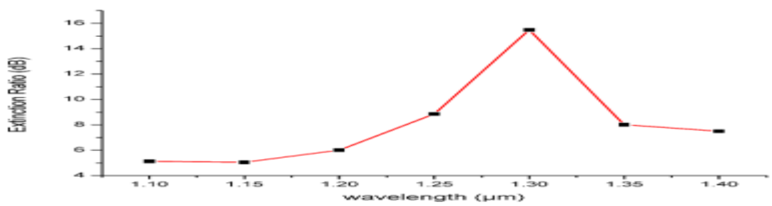

Figure 13 Extinction ratio vs. wavelength

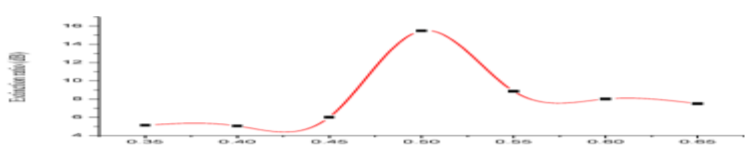

Figure 14 Extinction ratio vs. coupling ratio

The efficiency of a terminal is said to have an insertion loss if the amount of power it receives is less than the amount of power that is provided to it. Formalized Here:

$$IL\ (dB) = 10\log\left(\frac{P_{out}}{P_{in}}\right)$$

The 2 to 4 line decoder's ER and IL values are listed in Table 5.

Table 5 ER and IL for 2 to 4 line decoder

P_{min}^{1}	P_{max}^{0}	ER (dB)
0.9872	0.021	16.72186
P_{in}	P_{out}	Insersion loss (IL) dB
0.9989	0.9926	0.0274

Parameters such as ER and IL for decoders with 3-8 lines are listed in Table6

Table 6 ER and ILfor 3 to 8 line decoder

P_{min}^{1}	P_{max}^{0}	**ER (dB)**
0.9872	0.021	15.25
P_{in}	P_{out}	Insersion loss (IL) dB
0.9989	0.9926	0.0235

Table 7. displays estimated values for ER and IL for a 4 to 2 line encoder.

Table 7. Performance paramters for 4 to 2 Encoder

P_{min}^{1}	P_{max}^{0}	**ER (dB)**
0.9872	0.021	16.72186
P_{in}	P_{out}	IL (dB)
0.9999	0.9872	0.055514

CONCLUSION:

An encoder and decoder designed using a combinational circuit are demonstrated. Here, we have a look at the stats for the 2-4 line encoders and decoder, as well as the 4-2 line device. Losses inside the system must be kept to a minimum, and other critical parameters must also be maintained, for the system to be considered successful. Optical communication system factors including extinction ratio, cross talk, and insertion loss are computed and analyzed in the findings and discussion section. The similar calculation for a 2–4 line decoder yields the number 16.7218 for the extinction ratio, which should be high. As compared to logic devices based on SOA-MZI, this ER value is rather high. The insertion loss was also determined to be 0.0274 dB and was found to be optimally low. The ER and IL of a 3-8 line decoder are similarly determined to be 15.25 dB and 0.0235 dB, respectively. For the encoder, we get an ER of 16.7218 dB and an IL of 0.05551 dB. It is shown how the proposed devices would be laid out and analyzed mathematically and positive findings from MATLAB simulations are presented as well.

REFERENCES:

[1] Witkowska, S. G. Leon-Saval, A. Pham, and T. A. Birks, “All-fiber LP11 mode converters,” Opt. Lett. 33, 306–308 (2008).

[2] Borghesani, A. (2007). Optoelectronic Components for WDM-PON. 305 - 308. 10.1109/ICTON.2007.4296094.

[3] Chanderkanta, & Chen, Nan-Kuang & Kaushik, Brajesh Kumar & Kumar, Santosh. (2019). Implementation of reversible Peres gate using electro-optic effect inside lithium-niobate based Mach-Zehnder interferometers. Optics & Laser Technology. 117. 28-37. 10.1016/j.optlastec.2019.04.007.

[4] Dewra, Sanjeev & Kaler, R S. (2013). Performance analysis of optical network based on optical add drop multiplexers with different MZI techniques. Optik - International Journal for Light and Electron Optics. 124. 347–351. 10.1016/j.ijleo.2011.12.060.

[5] E. P. Kokanyan, V. G. Babajanyan and G. G. Demirkhanyan, J. B. Gruber and S. Erdel, "Periodically poled structures in doped lithium niobate crystals," J. Appl. Phys. 92(3), 1544-1547 (2002).

[6] G. F. Li, N. Bai, N. B. Zhao, and C. Xia, "Space-division multiplexing: the next frontier in optical communication," Adv. Opt. Photon. 6, 413– 487 (2014).

[7] H. S. Chen, V. Sleiffer, F. Huijskens, R. van Uden, C. Okonkwo, P. Leoni, M. Kuschnerov, L. C. Nielsen, Y. Sun, H. de Waardt, and T. Koonen, "Employing prism-based three-spot mode coupler for high capacity MDM/WDM transmission," IEEE Photon. Technol. Lett. 24, 2474–2477 (2013).

[8] J. L. Dong, K. S. Chiang, and W. Jin, "Compact three-dimensional polymer waveguide mode multiplexer," J. Lightwave Technol. 33, 4580–4588 (2015).

[9] K. K. Wong, Properties of Lithium Niobate: EMIS Datareviews Series No. 28 (INSPEC, London, 2002). 48. M. Nakamura, M. Sekita, S. Takekawa and K. Kitamura, "Crystal growth and characterization of Nd, Mg co-doped near-stoichiometric LiNbO3," J. Cryst. Growth 290(1), 144-148 (2006).

[10] Lin, Y., Abel, P. R., Heller, A. and Mullins, C. B., "α-Fe2O3 Nanorods as Anode Material for Lithium Ion Batteries," J. Phys. Chem. Lett., 2, 2885–2891 (2011).

[11] Mohammed, Nazmi & ABo Elnasr, Huda & Aly, Moustafa & Member, Osa. (2012). Performance Evaluation and Enhancement of 2×2 Ti: $LiNbO_3$ Mach Zehnder Interferometer Switch at 1.3 µm and 1.55 µm. Performance Evaluation of FSO Link Under NRZ-RZ Line Codes, Different Weather Conditions and Receiver Types in the Presence of Pointing Errors. 6. 36-49.

[12] N. P. Diamantopoulos, M. Hayashi, Y. Yoshida, A. Maruta, R. Maruyama, N. Kuwaki, K. Takenaga, H. Uemura, S. Matsuo, and K. Kitayama, "Mode-selective optical packet switching in mode-division multiplexing networks," Opt. Express 23, 23660–23666 (2015).

[13] T. Sun, L. Dai, C. Xu, Z. Qian, D. Li, J. Lin, R. Wang and Yuheng Xu, "Enhancement of nonvolatile holographic storage properties in In:Ce:Mn:$LiNbO_3$ crystal by

July /August 2020
ISSN: 0193-4120 Page No. 6801-6817

[Li]/[Nb] ratios," J. Mol. Struc. 1053(5), 1-4 (2013).

[14] W. Jin and K.S. Chiang,"Mode switch based on electro-optic long-period waveguide grating in lithium niobate," Opt. Lett. 40, 237–240 (2015).

[15] Zhang, J. Huang, T., Liu, Z., Yu, A., Mesoporous Fe_2O_3 nanoparticles as high-performance anode materials for lithium-ion batteries, Electrochem. Commun., 29, 17–20 (2013).